Strain-Balanced $In_{0.57}Ga_{0.43}As$ p-i-n Photodiodes for High-Sensitivity Extended SWIR Detection

Sungun Baek[1], Yeong In Song[1], and Jae Cheol Shin[1,2,*]

[1] Department of electronics and electrical engineering, Dongguk University-Seoul, 30 Pildong-ro 1-gil Jung-gu, Seoul 04620 South Korea

[2] EPI Solution, Inc., 109 Gwanggyo-ro, Yeongtong-gu, Suwon-si, Gyeonggi-do 16229, South Korea

[*]Corresponding author (jcshin@dgu.ac.kr)

Abstract

This study demonstrates the development of an $In_{0.57}Ga_{0.43}As$ pin photodiode on an InP substrate, specifically engineered for extended short-wave infrared (SWIR) detection up to 1.75 μm. To mitigate the 0.3% compressive strain inherent in the $In_{0.57}Ga_{0.43}As$ active region, a strain-balancing architecture incorporating multiple tensile-strained $In_xGa_{1-x}As$ layers were strategically implemented. This approach successfully reduced the net residual strain to below 0.1%, resulting in a 1-μm-thick, dislocation-free active region. The fabricated device exhibited a peak responsivity of 0.9 A/W at 1.55 μm and maintained high performance at extended wavelengths, yielding 0.6 A/W at 1.7 μm and 0.3 A/W at 1.75 μm. These values represent state-of-the-art performance in the 1.7 μm regime for non-metamorphic InGaAs material systems, validating the effectiveness of the proposed strain-compensated design for high-sensitivity SWIR applications.

Keywords: Short-Wave Infrared (SWIR), Strain Compensation, Photodiode, $In_xGa_{1-x}As$,

Metal-Organic Chemical Vapor Deposition (MOCVD)

Introduction

High-performance photodetectors operating in the short-wave infrared (SWIR) spectrum are pivotal for a diverse range of applications, including fiber-optic communications, industrial sensing, and advanced surveillance.[1-4] Among various semiconductor candidates, $In_xGa_{1-x}As$ has emerged as the premier material for this spectral range due to its exceptional electron mobility and the versatility offered by its tunable bandgap.[5] Conventionally, $In_{0.53}Ga_{0.47}As$ lattice-matched (LM) to InP substrates is utilized, providing a bandgap energy of approximately 0.75 eV at room temperature, which corresponds to a detection cutoff wavelength of approximately 1.65 μm.

However, there is an increasing demand to extend detection capabilities beyond this conventional limit, particularly toward the 1.75 μm wavelength region. Extending the spectral response to 1.75 μm offers two critical advantages. First, this region is rich in the molecular absorption fingerprints of various organic compounds, including C-H, O-H, and N-H bonds. Consequently, sensitivity in this range is essential for developing next-generation gas sensors and ultra-high-resolution medical imaging systems, such as optical coherence tomography (OCT), which require deep tissue penetration and molecular specificity.[6-10] Second, the 1.75 μm wavelength exhibits superior atmospheric and material penetration compared to standard near-infrared (NIR) light. It can effectively bypass environmental obscurants such as fog and smoke, and penetrate materials like polymer packaging and silicon wafers, providing substantial benefits for industrial quality inspection and secure communications under challenging conditions.[11]

To achieve a detection wavelength of 1.75 μm in $In_xGa_{1-x}As$, the Indium mole fraction must be increased to approximately $x = 0.57$. However, growing $In_{0.57}Ga_{0.43}As$ directly on a standard

InP substrate introduces a significant lattice mismatch. This mismatch generates considerable elastic strain within the material, which, if unmanaged, triggers the formation of misfit dislocations that severely degrade device reliability and quantum efficiency.

The traditional strategy to mitigate this lattice incompatibility is the implementation of a metamorphic buffer layer (MBL) to bridge the lattice constant jump.[12-14] While MBLs facilitate strain relaxation, the process of accommodating a significant lattice parameter difference inevitably generates a high density of threading dislocations (TDs) and associated crystalline defects. These defects act as potent Shockley-Read-Hall (SRH) recombination centers and facilitate trap-assisted tunneling, which dramatically increases the dark current. For PIN photodiodes (PIN PDs), maintaining a low dark current is fundamental to achieving a high signal-to-noise ratio (SNR) and high specific detectivity (D*).[15] Because PIN PDs rely on a high-quality depletion region for efficient carrier collection, the presence of dislocations makes the fabrication of high-imaging-quality MBL-based devices notoriously difficult. The resulting performance degradation remains a major impediment to developing the high-sensitivity, extended-wavelength $In_xGa_{1-x}As$ photodetectors required for demanding industrial and medical applications. Therefore, a novel approach to realize high-quality, strain-relaxed $In_{0.57}Ga_{0.43}As$ on InP substrates—one that fundamentally minimizes the formation and propagation of crystalline defects—is urgently needed.

In this work, we propose strain-balanced architecture for $In_xGa_{1-x}As$-based photodetectors operating at 1.7 μm and beyond. To extend the absorption limit, the Indium composition was increased to 0.57, introducing compressive strain in the active region. To compensate for this, we strategically incorporated tensile-strained InGaAs layers within the active region design. As a result, a misfit-dislocation-free active region for 1.7 μm detection and beyond was successfully grown on an InP substrate. The developed PIN PD demonstrates state-of-the-art performance, providing a robust and scalable solution for high-sensitivity extended-SWIR

sensing.

Experimental Methods

PIN photodiode structures were grown on heavily doped n-type InP substrates (1–3 x 10^{18} cm^{-3}) using a metal–organic chemical vapor deposition (MOCVD) system (AIXTRON A200). Trimethylindium (TMIn) and trimethylgallium (TMGa) were used as group-III precursors, while arsine (AsH_3) and phosphine (PH_3) served as group-V sources. The growth was carried out at 650 °C under a reactor pressure of 100 mbar. Silane (SiH_4) and diethylzinc (DEZn) were employed as n-type and p-type dopants, respectively. High-resolution X-ray diffraction (XRD) measurements confirmed that the $In_xGa_{1-x}As$ layers were lattice-matched to the InP substrate.

For metallization, AuGe/Ni/Au and Ti/Pt/Au were deposited as n- and p-type contacts, respectively, followed by rapid thermal annealing (RTA) to achieve low-resistance ohmic characteristics.

Electrical evaluations were performed at 300 K using a semiconductor parameter analyzer (Keithley 4200-SCS). Current–voltage (I–V) measurements were conducted to analyze the dark current and junction characteristics. The photocurrent was measured under illumination from a reference laser diode emitting at 1550 nm.

Spectral responsivity was characterized using a monochromator (Newport CS260), providing wavelength-selective illumination from 1000 to 1800 nm. A calibrated germanium (Ge) detector was used to monitor incident optical power, ensuring accurate responsivity measurements.

Results and Discussion

The fundamental challenge in extending the spectral reach of InGaAs-based detectors on InP substrates lies in the management of elastic strain energy. As the indium mole fraction is increased to 0.57 to narrow the bandgap, a compressive strain of approximately 0.3% is inevitably introduced due to lattice mismatch with the InP substrate. According to the Matthews–Blakeslee criterion, this strain severely limits the critical thickness to a value far below that required for efficient photon absorption in the short-wave infrared (SWIR) band.[16-18] Consequently, simply increasing the thickness of the In-rich InGaAs absorption layer leads to the formation of misfit dislocations, which significantly degrade both material quality and device performance. To overcome this fundamental limitation without resorting to defect-prone metamorphic buffer layers (MBLs), we implemented a step-graded, strain-balanced epitaxial architecture. In this approach, compressively strained $In_{0.57}Ga_{0.43}As$ absorption layers were strategically interleaved with tensile-strained $In_xGa_{1-x}As$ layers ($x < 0.53$). This configuration establishes an effective strain-compensation mechanism in which opposing strain components cancel each other. As a result, the overall strain-thickness product of the epitaxial stack is maintained near zero, thereby suppressing both the nucleation and propagation of misfit dislocations. This strategy enables the realization of a thick absorption region while preserving high crystalline quality and structural stability.

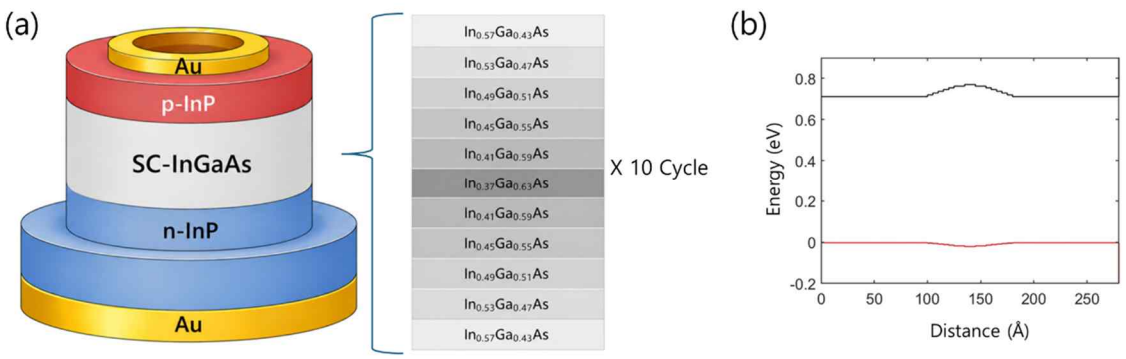

Figure 1. (a) Schematic device structure and (b) energy band diagram of a strain-balanced

$In_{0.57}Ga_{0.43}As$ p-i-n photodiode

The device structure, illustrated in Fig. 1(a), was carefully engineered to optimize electrical performance, particularly by minimizing leakage current. An InP layer was employed as the top contact layer, leveraging its wide bandgap to effectively suppress surface leakage currents. To further extend the detection wavelength, the active region incorporates six distinct $In_xGa_{1-x}As$ alloy compositions (x = 0.57, 0.53, 0.49, 0.45, 0.41, and 0.37), as shown in Fig. 1(a). While $In_{0.57}Ga_{0.43}As$ enables long-wavelength absorption, it introduces substantial compressive strain (~0.3%) on the InP substrate. To compensate for this, tensile-strained InGaAs layers with lower indium content (x = 0.49-0.37) were incorporated in a step-graded configuration, as depicted in Fig. 1(b).

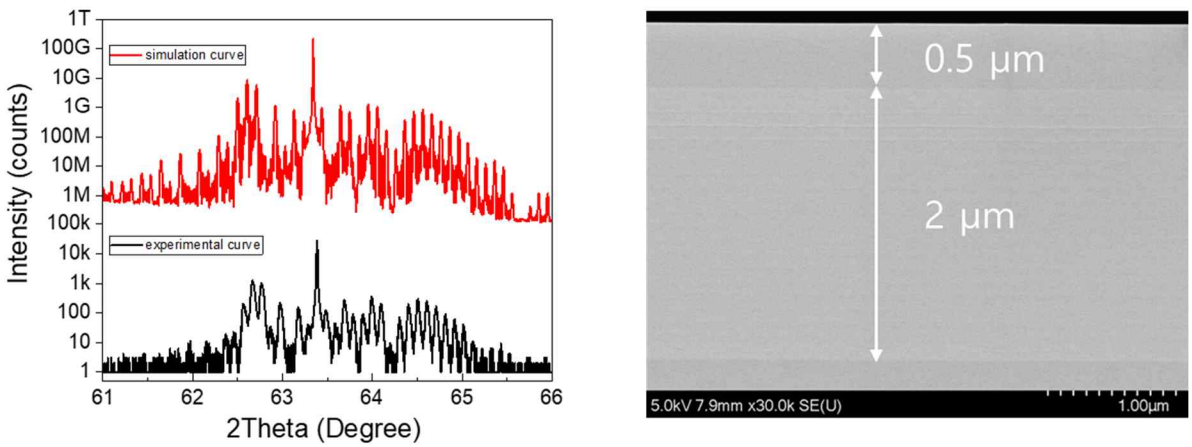

Figure 2. (a) Simulated and experimental XRD spectra and (b) cross-sectional SEM image of the strain-balanced $In_{0.57}Ga_{0.43}As$ p-i-n photodiode

This gradual compositional transition not only balances the strain but also mitigates abrupt band discontinuities, thereby facilitating efficient carrier transport across the heterointerfaces. As a result of this strain-engineered design, the net residual strain of the entire epitaxial structure is reduced to below 0.05%, as confirmed by high-resolution X-ray diffraction (XRD) analysis in Fig. 2(a). The XRD rocking curves exhibit well-defined satellite peaks, indicating excellent periodicity and high crystalline quality across the multilayer stack. Cross-sectional scanning electron microscopy (SEM) images, shown in Fig. 2(b), further verify the absence of noticeable threading dislocations, even for a total $In_{0.57}Ga_{0.43}As$ thickness of 1 μm. This thickness provides a sufficiently long optical path length to absorb over 90% of incident photons beyond 1.75 μm, while maintaining a low-defect environment critical for minimizing noise and ensuring high device reliability.

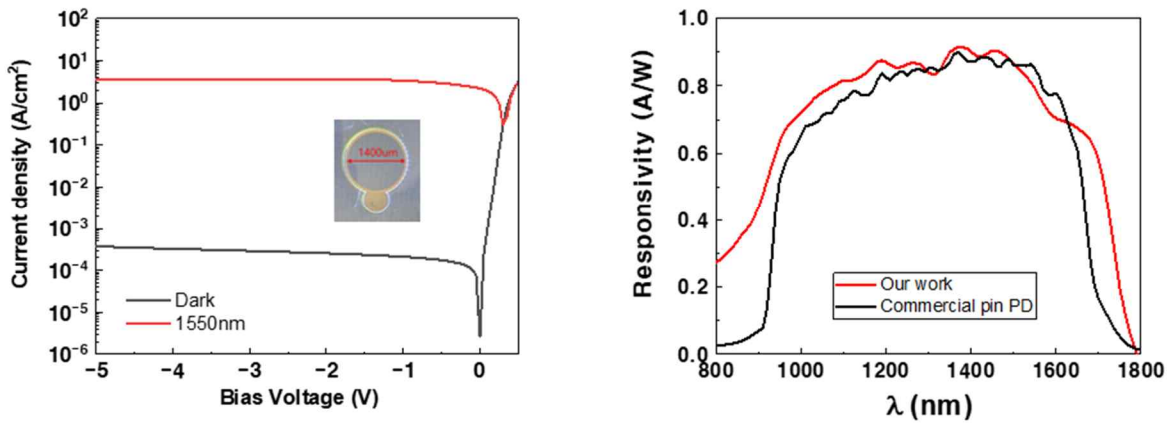

Figure 3. (a) Dark and light current density-voltage (J-V) characteristics of the strain-balanced $In_{0.57}Ga_{0.43}As$ p-i-n photodiode. (b) Spectral responsivity of the fabricated device compared with a commercial InGaAs-based pin photodiode in the near-infrared (NIR) region

The electrical and optical characteristics of the strain-balanced device demonstrate a

significant performance enhancement compared to conventional lattice-matched (LM) detectors. As shown in Fig. 3(a), the device exhibits a dark current density on the order of 10^{-4} A/cm^2 and a photocurrent density on the order of 3.5 A/cm^2 under 1.55 μm illumination. Under reverse bias, the device shows stable current–voltage (I–V) characteristics with low leakage current, indicating effective suppression of Shockley–Read–Hall (SRH) recombination and the high shunt resistance further confirms the superior material quality. The slightly elevated dark current compared to state-of-the-art InGaAs p-i-n photodiodes is primarily attributed to the no passivation process for the dangling bonding from side-wall of the mesa structure as shown in Fig.1(a). Despite this, the device maintains excellent photoresponse characteristics. As shown in Fig. 3(b), the device exhibits high responsivity across both the standard SWIR and extended-SWIR regions. A responsivity of 0.9 A/W at 1.55 μm was achieved, comparable to that of state-of-the-art LM photodiodes, indicating that the strain-engineered architecture does not compromise baseline device efficiency. The commercial LM photodiode used for comparison was a commercially available device. Furthermore, the responsivity remains consistently high across the measured spectral range, reflecting uniform carrier generation and efficient carrier collection throughout the active region. This broadband response originates from the compositional diversity of the active region. While the $In_{0.57}Ga_{0.43}As$ layers are primarily responsible for absorbing longer-wavelength photons (up to 1.75 μm), the tensile-strained InGaAs layers with higher Ga content possess wider bandgaps and contribute to absorption in the shorter wavelength region. This synergistic interaction enables a broad and extended quantum efficiency across the SWIR spectrum. Notably, the device maintains a responsivity of approximately 0.8 A/W at 1.7 μm and 0.4 A/W at 1.75 μm, significantly outperforming conventional lattice-matched $In_{0.53}Ga_{0.47}As$ photodiodes, which exhibit a sharp responsivity cutoff near 1.65 μm. These results represent one of the highest responsivities reported near 1.7 μm for InGaAs-on-InP systems, highlighting the effectiveness of the proposed strain-balanced

design.

Conclusion

In summary, we have demonstrated an $In_{0.57}Ga_{0.43}As$-based p-i-n photodiode with extended wavelength sensitivity up to 1.75 μm on an InP substrate. The proposed architecture achieves near-zero net strain, enables thick absorption layers without dislocation formation, and delivers superior optical performance compared to conventional approaches. This work provides a robust and scalable pathway for realizing high-performance SWIR photodetectors for advanced sensing, imaging, and defense applications.

Acknowledgement

This work was supported by the Agency for Defense Development by the Korean Government (Grant No. UI230018TD). It was also supported by the Technology Innovation Program (RS-2023-00235844, 1415187621) for the "Development of nano-structured materials and devices for super steep subthreshold swing," funded by the Ministry of Trade, Industry & Energy (MOTIE, Korea), and by the National Research Foundation of Korea (NRF) (RS-2025-23963217).

REFERENCES

(1) Şahin, A.; Gül, M. S.; Uzgur, F.; Kocaman, S. Dual-band InGaAs nBn photodetectors at 2 μm. *Applied Physics Letters* **2022**, *120* (9). DOI: 10.1063/5.0080950 (acccessed 2/25/2026).

(2) Rutz, F.; Aidam, R.; Bächle, A.; Heußen, H.; Bronner, W.; Rehm, R.; Benecke, M.; Sieck, A.; Brunner, S.; Göhler, B.; et al. *InGaAs-based SWIR photodetectors for night vision and gated viewing*; SPIE, 2018.

(3) Cao, J.; Yu, Y.; Li, T.; Yu, C.; Gu, Y.; Yang, B.; Ma, Y.; Shao, X.; Li, X.; Gong, H. Lightly doped In0.53Ga0.47As/InP SWIR photodetectors with diffusion barrier structure. *Infrared Physics & Technology* **2024**, *137*, 105112. DOI: https://doi.org/10.1016/j.infrared.2023.105112.

(4) Li, X.; Zhang, J.; Yue, C.; Tang, X.; Gao, Z.; Jiang, Y.; Du, C.; Deng, Z.; Jia, H.; Wang, W.; et al. High performance visible-SWIR flexible photodetector based on large-area InGaAs/InP PIN structure. *Scientific Reports* **2022**, *12* (1), 7681. DOI: 10.1038/s41598-022-11946-7.

(5) Goetz, K. H.; Bimberg, D.; Jürgensen, H.; Selders, J.; Solomonov, A. V.; Glinskii, G. F.; Razeghi, M. Optical and crystallographic properties and impurity incorporation of $Ga_xIn_{1-x}As$ ($0.44<x<0.49$) grown by liquid phase epitaxy, vapor phase epitaxy, and metal organic chemical vapor deposition. *Journal of Applied Physics* **1983**, *54* (8), 4543-4552. DOI: 10.1063/1.332655 (acccessed 2/25/2026).

(6) Kawagoe, H.; Ishida, S.; Aramaki, M.; Sakakibara, Y.; Omoda, E.; Kataura, H.; Nishizawa, N. Development of a high power supercontinuum source in the 1.7 μm wavelength region for highly penetrative ultrahigh-resolution optical coherence tomography. *Biomed. Opt. Express* **2014**, *5* (3), 932-943. DOI: 10.1364/BOE.5.000932.

(7) Paul, C.; Ed, A. D. A.; John, P. D. Theoretical analysis of a methane gas detection system, using the complementary source modulation method of correlation spectroscopy. *Measurement Science and Technology* **2004**, *15* (8), 1629. DOI: 10.1088/0957-0233/15/8/034.

(8) Wang, S.; Jiang, H.; Wang, B.; Du, J.; Wang, S.; Qin, L. A technique for detecting hydrogen and methane using refractive index sensitivity. *Process Safety and Environmental Protection* **2024**, *188*, 781-792. DOI: https://doi.org/10.1016/j.psep.2024.05.131.

(9) Bashkatov, A. N.; Genina, E. A.; Kochubey, V. I.; Tuchin, V. V. Optical properties of human skin, subcutaneous and mucous tissues in the wavelength range from 400 to 2000 nm. *Journal of Physics D: Applied Physics* **2005**, *38* (15), 2543. DOI: 10.1088/0022-3727/38/15/004.

(10) Sharma, U.; Chang, E. W.; Yun, S. H. Long-wavelength optical coherence tomography at 1.7 μm for enhanced imaging depth. *Opt. Express* **2008**, *16* (24), 19712-19723. DOI: 10.1364/OE.16.019712.

(11) Ijaz, M.; Ghassemlooy, Z.; Minh, H. L.; Rajbhandari, S.; Perez, J. Analysis of fog and smoke attenuation in a free space optical communication link under controlled laboratory conditions. In *2012 International Workshop on Optical Wireless Communications (IWOW)*, 22-22 Oct. 2012, 2012; pp 1-3. DOI: 10.1109/IWOW.2012.6349680.

(12) Swaminathan, K.; Yang, L. M.; Grassman, T. J.; Tabares, G.; Guzman, A.; Hierro, A.; Mills, M. J.; Ringel, S. A. Metamorphic In0.20Ga0.80As p-i-n photodetectors grown on GaAs substrates for near infrared applications. *Opt. Express* **2011**, *19* (8), 7280-7288. DOI: 10.1364/OE.19.007280.

(13) Kirch, J.; Garrod, T.; Kim, S.; Park, J. H.; Shin, J. C.; Mawst, L. J.; Kuech, T. F.; Song, X.; Babcock, S. E.; Vurgaftman, I.; et al. InAsyP1−y metamorphic buffer layers on InP substrates for mid-IR diode lasers. *Journal of Crystal Growth* **2010**, *312* (8), 1165-1169. DOI: https://doi.org/10.1016/j.jcrysgro.2009.12.057.

(14) Hayat, M. M.; Saleh, B. E. A.; Teich, M. C. Effect of dead space on gain and noise of double-carrier-multiplication avalanche photodiodes. *IEEE Transactions on Electron Devices* **1992**, *39* (3), 546-552. DOI: 10.1109/16.123476.

(15) Wang, H.; Gu, Y.; Yu, C.; Zhu, S.; Zhu, Y.; Chen, P.; Cao, J.; Yang, B.; Li, T.; Shao, X.; et al. Direct correlation of defects and dark currents of InGaAs/InP photodetectors. *Materials Science in Semiconductor Processing* **2021**, *123*, 105540. DOI: https://doi.org/10.1016/j.mssp.2020.105540.

(16) Salviati, G.; Ferrari, C.; Lazzarini, L.; Nasi, L.; Drigo, A. V.; Berti, M.; De Salvador, D.; Natali, M.; Mazzer, M. Structural characterization of InGaAs/InP heterostructures grown under compressive and tensile stress. *Applied Surface Science* **2002**, *188* (1), 36-48. DOI: https://doi.org/10.1016/S0169-4332(01)00726-7.

(17) Gendry, M.; Drouot, V.; Santinelli, C.; Hollinger, G. Critical thicknesses of highly strained InGaAs layers grown on InP by molecular beam epitaxy. *Applied Physics Letters* **1992**, *60* (18), 2249-2251. DOI: 10.1063/1.107045 (acccessed 2/25/2026).

(18) Bennett, B. R.; Alamo, J. A. d. High quality InGaAs/InP and InAlAs/InP heterostructures beyond the Matthews-Blakeslee critical layer thickness. In *LEOS 1992 Summer Topical Meeting Digest on Broadband Analog and Digital Optoelectronics, Optical Multiple Access Networks, Integrated Optoelectronics, and Smart Pixels*, 21-24 April 1992, 1992; pp 650-653. DOI: 10.1109/ICIPRM.1992.235553.